

Received 13 July 2024, accepted 5 August 2024, date of publication 12 August 2024, date of current version 21 August 2024.

Digital Object Identifier 10.1109/ACCESS.2024.3442230

## RESEARCH ARTICLE

# Road Incident Detection Under Rate Adaptation-Based Congestion Control in Cooperative Vehicular Systems

SANDY BOLUFÉ<sup>1</sup>, (Member, IEEE), JORGE F. SILVA<sup>2,3</sup>, (Senior Member, IEEE), CESAR A. AZURDIA-MEZA<sup>2</sup>, (Member, IEEE), ISMAEL SOTO<sup>1</sup>, (Senior Member, IEEE), AND SANDRA CÉSPEDES<sup>3,4</sup>, (Senior Member, IEEE)

<sup>1</sup>Department of Electrical Engineering, University of Santiago of Chile (USACH), Santiago 9170124, Chile

<sup>2</sup>Department of Electrical Engineering, University of Chile (UCHILE), Santiago 8370451, Chile

<sup>3</sup>Advanced Center for Electrical and Electronic Engineering (AC3E), Federico Santa María Technical University (UTFSM), Valparaíso 2390136, Chile

<sup>4</sup>Department of Computer Science and Software Engineering, Concordia University, Montreal, QC H3G 1M8, Canada

Corresponding author: Sandy Bolufé (sandy.bolufe@usach.cl)

This work was supported in part by the Advanced Center for Electrical and Electronic Engineering (AC3E)–ANID Basal Project under Grant FB0008, in part by the ANID FONDECYT Postdoctorado under Grant 3230047, in part by the FONDECYT Project under Grant 1211132, in part by the Cooperation Program STIC-AMSUD under Grant AMSUD220026, in part by the FRDP Start-Up Funds Gina Cody School Concordia University, and in part by the DICYT/USACH under Grant 062413SG.

**ABSTRACT** Cooperative vehicular systems require that vehicles fuse sensor data and broadcast one-hop safety messages containing their kinematic information to enable vehicular applications based on incident detection. Several congestion control mechanisms have been proposed to mitigate channel congestion resulting from the continuous transmission of safety messages. This paper investigates the effect of message rate adaptation-based congestion control from a road safety perspective by evaluating the feasibility of prominent approaches, such as PULSAR, LIMERIC, reactive ETSI DCC, and SAE J2945/1, to support lane-changing maneuvers on multi-lane highways under varying conditions. Simulation results demonstrate that message size, vehicular density, losses at the physical layer, and observation time significantly influence the lane-changing application's capability to detect unsafe maneuvers when congestion control is in action. Specific recommendations and guidelines for congestion control are provided to improve decision-making at the application level.

**INDEX TERMS** Congestion control, cooperative vehicular systems, ETSI DCC, incident detection, lane-changing maneuver, LIMERIC, PULSAR, road safety applications, SAE J2945/1, vehicular density.

## I. INTRODUCTION

Cooperative vehicular systems (CVS) are rapidly progressing and will soon significantly reduce road traffic accidents [1], [2], [3]. Automobile manufacturers already include an increasing number of embedded sensors (e.g., lidars, radars, and cameras) in modern vehicles with the aim of effectively detecting potential threats in the proximity [4], [5], [6]. As a complement to sensors, vehicles are also equipped with wireless communication technologies to increase their perception of the surrounding traffic [7], [8], [9]. Two key

radio access technologies for vehicle-to-everything (V2X) communications are Dedicated Short Range Communications (DSRC) [10], which have led to the new standard IEEE 802.11bd [11], and Cellular V2X (C-V2X), which includes 4G Long Term Evolution (LTE) V2X and the recent 5G New Radio (NR) V2X [8], [12]. DSRC is based on the IEEE 802.11p standard, which employs the Carrier Sense Multiple Access with Collision Avoidance (CSMA/CA) protocol to coordinate access to the communication channel [10], [13]. In C-V2X, vehicles can operate outside network coverage by autonomously selecting their communication resources [8], [12]. IEEE 802.11bd and 5G NR V2X have been developed by the automotive industry and research

The associate editor coordinating the review of this manuscript and approving it for publication was Binit Lukose<sup>1b</sup>.

community to support enhanced V2X services [14]. The integration of detection sensors and V2X communications is crucial for enabling future connected and autonomous vehicles [15].

In CVS, vehicles periodically transmit one-hop broadcast messages, called Basic Safety Messages (BSMs) [16] in the U.S. and Cooperative Awareness Messages (CAMs) [17] in Europe, that contain kinematic information such as position, speed, acceleration, and heading. These safety messages are the basis for enabling real-time road safety applications relying on vehicle-to-vehicle (V2V) communications for incident detection in different vehicular scenarios [6], [7], [17]. Lane-changing is a safety-relevant vehicular scenario addressed by the Society of Automotive Engineers (SAE) and the European Telecommunication Standards Institute (ETSI) in SAE J2945/1 [18] and ETSI TS 101 539-3 [19], respectively. Lane-changing maneuvers are challenging and can contribute to merging conflicts and traffic accidents [20], [21]. Consequently, V2V-based lane-changing applications should utilize the kinematic information from received messages to avoid potential collisions between target vehicles [18], [19]. In some cases, the perception capabilities of vehicles can be improved by using V2V communications to exchange not only local kinematic parameters but also sensing information (e.g., from the onboard detection sensors) in the form of Collective Perception Messages (CPMs), as specified in ETSI TR 103 562 [22]. Fused data from detection sensors can be affected by in-vehicle faults and interferences, which may propagate to safety-related applications and impair decision-making [23].

A critical concern is the channel congestion arising from the regular transmission of safety messages. In contrast to C-V2X, where the study of congestion control is relatively new [8], [24], congestion mitigation for V2V communications based on IEEE 802.11p has been further investigated [18], [25], [26], [27]. Congestion control typically adapts the transmission parameters (e.g., message rate, transmission power, and/or data rate) of safety messages in vehicles to maintain the channel load below a certain target threshold [28]. Congestion control based on transmission power adaptation can lead to inadequate warning distances for different vehicular contexts because the transmission power usually depends on the channel load (i.e., vehicle dynamics are not considered). On the other hand, the data rate has a significant influence on packet losses in both medium-access control (MAC) and physical (PHY) layers. The data rate determines the time a safety message is sent on the communication channel, which is directly related to packet collisions at the MAC layer [29]. The data rate could also degrade the message reception probability due to PHY properties because a higher data rate is more prone to interference and requires a higher receive threshold [13]. These issues pose a challenge to isolating the effect that congestion control based on the adaptation of transmission power and data rate may have on road safety applications.

The adaptation of the message rate is a relevant dimension within the congestion control approaches standardized by SAE and ETSI in [18] and [19], respectively. Message rate adaptation-based congestion control focuses on adjusting the vehicle transmission rate of safety messages to directly regulate channel utilization without affecting the transmission range or modulation scheme. Given the importance of standardized message rate adaptation-based congestion control for the proper performance of CVS, as well as the challenge of isolating the effect of congestion control based on the adaptation of transmission power and data rate on safety applications, this work specifically focuses on analyzing the influence of message rate adaptation, leaving the study of power and data rate controls for future research. Prominent congestion control approaches that rely on the adaptation of message rate for IEEE 802.11p-based V2V communications have been proposed in the literature. In their work on Vehicle Safety Communications, Tielert et al. [25] presented the Periodically Update Load Sensitive Adaptive Rate (PULSAR) approach utilizing binary rate control with the Additive Increase Multiplicative Decrease (AIMD) technique for congestion management. Bansal et al. [26] proposed the LInear MESSage Rate Integrated Control (LIMERIC) algorithm, which aims to limit channel utilization and achieve fairness in message rate allocation among neighboring vehicles. On the other hand, ETSI has proposed a set of Decentralized Congestion Control (DCC) [27] mechanisms that adapt the transmission rate of vehicles to mitigate channel congestion. Two different rate adaptation-based approaches have been specified by ETSI. The adaptive approach, which is based on LIMERIC, and the reactive approach, which relies on a state machine. In the congestion control approach standardized by SAE J2945/1 [18], the transmission rate of safety messages in the vehicle is determined based on the number of nearby neighbors.

## A. CONTRIBUTION AND ORGANIZATION

Congestion control has been effective in controlling channel load, however, its influence on the decision-making process necessary for critical road safety tasks at the application level should be further investigated. To the best of our knowledge, the effect of congestion control has not been examined from the perspective of road safety.

This paper investigates the effect of prominent message rate adaptation-based congestion control approaches, such as PULSAR [25], LIMERIC [26], reactive ETSI DCC [27], and SAE J2945/1 [18], on the decision-making of road safety applications under varying conditions. Specifically, the capability of a lane-changing application relying on V2V communications based on IEEE 802.11p is evaluated to identify unsafe maneuvers using safety messages rate-limited by a congestion control mechanism. The analysis considers the influence of message size, vehicular density, safety message losses at the PHY level, and the time window in which the feasibility of the lane-changing maneuver is

evaluated. It is worth pointing out that the study focuses on assessing the impact of a congestion control mechanism on road safety rather than designing a complex safety application for accident prevention. As such, the lane-changing application employed in the evaluations follows a straightforward yet effective design. The design of more robust operation modes for road safety applications, including the lane-changing application, remains an open challenge that is outside the scope of this work.

The specific contributions of this study are summarized as follows:

- The effect of message rate adaptation-based congestion control is investigated from a road safety perspective, focusing on the decision-making process necessary for critical safety tasks at the application level.
- The lane-changing scenario is modeled considering unsafe maneuvers and incident detection based on position and motion state tracking utilizing kinematic data from received safety messages.
- The influence of message size and vehicular density, in conjunction with congestion control, on both the message rate of the approaching vehicle and the reception probability of the vehicle performing lane changing is studied, focusing on the IEEE 802.11p MAC layer. The impact of the application's time window and message losses at the PHY level on road safety is also investigated.
- The impact of standard message rate adaptation-based congestion control on the incident-detection capability of the V2V-based lane-changing application is evaluated under varying conditions.

The remainder of this paper is organized as follows. Section II reviews related work. Section III introduces the system model containing the in-vehicle unit architecture, the lane-changing scenario, and the lane-changing application. Section IV presents standard rate adaptation-based congestion control. The influence of congestion control on road safety is discussed in Section V. The overall findings and recommendations as well as conclusions are given in Sections VI and VII, respectively.

## II. RELATED WORK

This section overviews relevant state-of-the-art research into the design and evaluation of rate adaptation-based congestion control. It also addresses the motivations and objectives of this work as well as the significance of the studied congestion control approaches.

In [30], the capabilities of PULSAR, LIMERIC, and reactive ETSI DCC to control channel load and achieve a fair message rate allocation at urban intersections are evaluated. To achieve global fairness, the cooperation strategy used in PULSAR is applied to LIMERIC and reactive ETSI DCC. The simulation results presented in this paper show that the global fairness principle leads to soft transitions decreasing the convergence time and volatility. Simulation results also evidence that the state machine-based control mechanisms of

reactive ETSI DCC may impair communication performance in terms of information freshness and communication range. The performance of PULSAR and LIMERIC in computing the message rate of vehicles is evaluated in [31]. This work shows that the underlying AIMD algorithm of PULSAR is outperformed by LIMERIC in terms of convergence speed and stability.

In [7], the authors evaluate the performance of LIMERIC considering metrics such as position error, packet collision rate, packet delivery ratio (PDR), and end-to-end latency. The simulation experiment performed in this study shows that the underlying linear rate-control equation in LIMERIC produces unfairness in message rate allocation in noisy channel busy ratio (CBR) measurements even with gain saturation. Besides, it is shown that LIMERIC maximizes channel utilization at the cost of reducing communication reliability and it is not capable of guaranteeing a pre-defined position error. In [32], the authors examine the performance of the reactive ETSI DCC mechanisms to understand their respective points of strength and weakness, considering the stability, channel load, delay, and reachability. This simulation analysis has been conducted under a variety of channel load conditions based on link metrics. The authors provide concrete findings and hints to improve the overall performance of reactive ETSI DCC.

In [33], multi-hop forwarding in the context of decentralized congestion control is addressed. The authors focus on congestion-enabled forwarding to improve communication performance in terms of reliability and latency for mixed data traffic composed of single- and multi-hop packets with different priorities. LIMERIC is employed as the rate adaptation algorithm to adjust the message rate and ensure that the network load keeps below a pre-defined threshold of the bandwidth. In [34], the authors focus on effectively integrating awareness control with congestion control by not only adapting the message rate to limit channel load but also considering the surrounding traffic situation. The performance of the proposed approach is compared to other rate adaptation-based congestion control algorithms, including LIMERIC + PULSAR.

The adaptive variant of ETSI DCC is studied in [35]. The authors analyze how the chosen parameters for the control approach can lead to a slow speed of convergence and long periods of unfairness in message rate allocation in transitory situations. To improve the performance, the authors propose a modification to the underlying adaptive control mechanism. In [36], the authors provide a more detailed investigation into the impact of the parameters configuration of the adaptive ETSI DCC in steady state and transitory situations. Their simulation study shows that an incorrect selection of parameters can make the adaptive ETSI DCC approach ineffective. In [5], the authors assess the impact of both reactive and adaptive ETSI DCC on cooperative perception. The set of experiments in this work shows that congestion control can influence the perception and latency in connected and automated vehicles.

In [37], the authors present a data rate control method with adaptive traffic control based on LIMERIC. For this purpose, a formulation of CBR related to transmission probability and application reliability is developed. Realistic simulations are used to evaluate the performance of the proposed method in terms of end-to-end delay and packet error rate. In [38], the authors provide a review of the ETSI DCC mechanism with its advantages and limitations. Alternative solutions and approaches are outlined and classified according to different scenarios (e.g., platooning) and control parameters (e.g., transmission rate, transmission power, and data rate). In [39], a decentralized congestion management system is developed by adapting the message rate based on the exponential function. The simulation results presented in this work show that the use of the developed technique reduces the channel busy time and the total lost packets. In [40], rate adaptation-based congestion control is applied to a platooning scenario. This work shows that the performance and stability of the platoon can be maintained under high channel load conditions. In [41], the authors evaluate the performance of the reactive ETSI DCC approach. They highlight the channel capacity under-utilization and the communication quality degradation and also propose several design improvements to enhance its performance.

In [42], the authors study the feasibility of implementing the distributed congestion control algorithm introduced in the SAE J2945/1 standard on top of the C-V2X stack. The performance of the message rate and transmission power control mechanisms is evaluated in dense vehicular scenarios. From the evaluation, they identify areas for potential design enhancements and further investigation. In [43], the authors investigate the performance of the SAE J2945/1 congestion control approach in C-V2X communication environments. They find that the SAE J2945/1 algorithm exhibits an imbalance between message rate control and transmission power control during congestion. To address this, the authors propose adjusting the message transmission rate control to react more relaxedly to congestion, allowing transmission power control to contribute actively to overall congestion control. In [24], the SAE 2945/1 congestion control mechanism is used to compare the performance of V2V communications in freeway scenarios under different traffic densities and radio access technologies. A relevant finding of this research is that both the SAE 2945/1 congestion control and the communication technology can significantly impact the performance of V2V communications.

In [44], the authors propose a distributed congestion control method that adjusts the interval of safety messages to maximize the number of successful transmissions. Vehicles estimate the vehicular density in their vicinity, and based on the estimated density, they calculate an optimal message transmission interval to maximize the number of successful message receptions per second by vehicles located at a target distance. In [45], the authors present a distributed algorithm for the joint adaptation of transmit power and message rate for congestion and awareness control. This approach employs a

network utility formulation of the congestion control problem to induce a desired fairness notion and set different priorities for vehicles. In [46], the authors propose a congestion control strategy based on the adaptation of message rate for alleviating channel congestion and minimizing information loss. Simulations are used in this work to demonstrate the advantages of the proposed solution in terms of metrics such as message transmission rate, message reception rate, PDR, and information loss ratio.

In [47], a DCC strategy called Transmission Timing Control (TTC) is presented, which distributes transmissions over time to avoid channel contention and reduce channel load. In [48], the authors propose a cross-layer technique for controlling congestion in an Internet of Vehicles (IoV) network, considering throughput and buffer use. Finally, in [49], an adaptive CAM messaging algorithm based on the emerging methodology of the age of information (AoI) is presented to minimize the age-penalty function in a trajectory prediction application. These studies address congestion control from different angles highlighting the importance of underlying control mechanisms for the successful operation of vehicular systems.

## A. MOTIVATIONS AND OBJECTIVES

Although there are valuable works on congestion control in the literature, the influence of underlying congestion control mechanisms on the decision-making processes of road safety applications remains insufficiently explored. The studies on rate adaptation-based congestion control primarily focus on parameter adaptation or evaluating the approach's capability to control channel load and achieve fairness in message rate allocation, considering factors such as convergence speed and stability. While some works have evaluated the performance of congestion control in terms of metrics relevant to road safety, studying the incident detection effectiveness of road safety applications when running on top of congestion control is still missing.

The primary objective of CVS is to enable road safety applications based on incident detection to improve driving safety. Accordingly, congestion control approaches should not only mitigate channel congestion but also facilitate the correct operation of road safety applications. This study intends to take a step forward by providing a comprehensive analysis of the effect of congestion control on road safety. Unlike previous studies, this research focuses on determining how rate adaptation-based congestion control influences incident detection at the application level. The focus is on evaluating the performance of a lane-changing application that operates on top of prominent congestion control approaches, such as PULSAR, LIMERIC, reactive ETSI DCC, and SAE J2945/1. Interest is in gaining insights into the application's ability to detect unsafe maneuvers under varying conditions to understand the limitations of congestion control. The study also aims to provide recommendations for congestion control

to improve the incident detection capabilities of road safety applications.

### B. SIGNIFICANCE OF THE STUDIED APPROACHES

To achieve the goals, the performance of the lane-changing application is evaluated by comparing four prominent congestion control approaches: PULSAR [25], LIMERIC [26], reactive ETSI DCC [27], and SAE J2945/1 [18], which hold great importance and garner significant interest from the research community and the automotive industry. This work specifically emphasizes PULSAR and LIMERIC, as they are two of the most relevant congestion control approaches available in the literature. PULSAR is a pioneering approach that has stood out in the literature on congestion control. The importance of PULSAR is determined by its early contribution to congestion mitigation by adapting the message rate of safety messages in vehicles to limit channel load and ensure global fairness. LIMERIC is another pioneering and widely recognized message rate adaptation-based congestion control method that has considerably influenced the design and implementation of congestion control algorithms. It has served as a reference for subsequent research, including the adaptive congestion control technique specified by European standards [27]. Additionally, the reactive variant of ETSI DCC as well as SAE J2945/1 are considered, as they represent standardized solutions. The DCC mechanisms standardized in ETSI TS 102 687 [27] are pivotal to ensuring the reliable operation of CVS. The ETSI DCC mechanisms dynamically adjust the transmission parameters of vehicles to prevent communication degradation due to excessive channel load. The congestion control mechanism standardized in SAE J2945/1 is essential for maintaining scalability as the number of communicating vehicles increases. This method aims at preventing channel saturation by adjusting the transmission parameters of safety messages according to the number of neighboring vehicles.

## III. SYSTEM MODEL

This section presents the system model which comprises the in-vehicle unit architecture, the lane-changing scenario, and the lane-changing application.

### A. SYSTEM OVERVIEW

Vehicles are progressively including sensors, such as lidars, radars, and cameras, that locally perceive the driving environment [4], [5], [6]. However, the detection sensors are still impaired by obstacles (e.g., obstructions due to nearby vehicles on the road), illumination, and weather conditions. They have issues in determining the location of oncoming traffic successfully, and their detection capabilities are affected by the distance [4], [5], [6]. To complement the operation of sensors, vehicles are equipped with wireless communication devices to increase their perception of the surrounding traffic [12], [14]. The premise is that by knowing the movement state of their neighbors, vehicles are better able for decision-

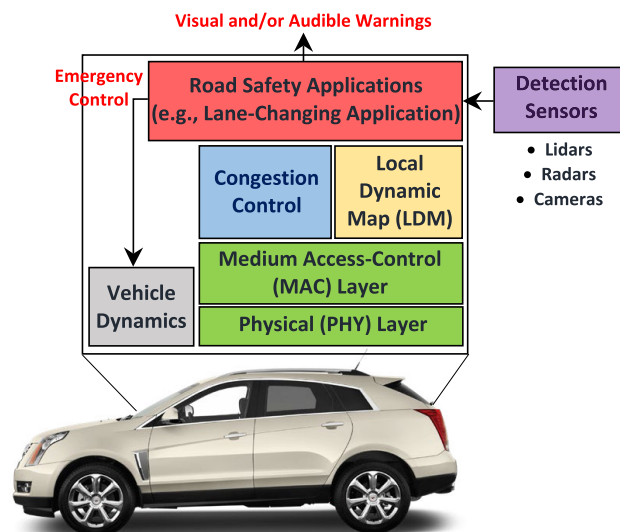


FIGURE 1. In-vehicle unit architecture devised from a road safety viewpoint.

making in hazardous situations [18], [19]. Thus, to make neighbors aware of their presence, vehicles regularly broadcast one-hop safety messages (i.e., BSMs [16] or CAMs [17]) including their kinematic information (e.g., position, speed, acceleration, heading, and other relevant data). The exchange of motion-state information allows creating a knowledge database with information on the dynamics of surrounding vehicles [17]. Then, kinematic information is employed by road safety applications to mitigate potential threats in real time [6], [7].

### B. IN-VEHICLE UNIT ARCHITECTURE

To better understand the relationship between the different components from a road safety perspective, the in-vehicle unit architecture as shown in Fig. 1 is devised. This custom architecture visualizes that decision-making of road safety applications, such as the lane-changing application, relies on kinematic information obtained from neighbors through V2V communications, which in turn, depends on congestion control. Road safety applications can also employ the information obtained through sensors to detect threats in the proximity of the vehicle.

In Fig. 1, the PHY and MAC layers are defined by vehicular communication technology, for example, based on IEEE 802.11p [10], [13]. Vehicle dynamics contain onboard sensors that produce vehicle motion state measurements (e.g., velocity, acceleration, and heading) and a Global Positioning System (GPS) receiver that provides positioning information [6], [7]. The Local Dynamic Map (LDM) database stores motion state information from surrounding vehicles, which is utilized to detect potential threats (e.g., a dangerous situation can be detected by tracking the position and movement state of vehicles) [6], [17]. If an imminent danger is identified, road safety applications provide visual and/or audible warnings to drivers in human-driven vehicles

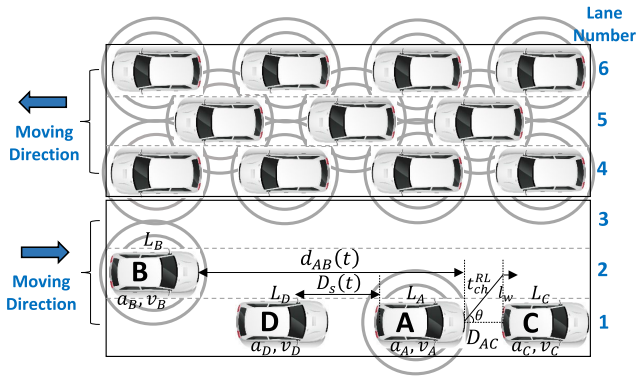


**FIGURE 2.** Lane-changing scenario. Vehicle A intends to change from lane 1 to lane 2 while B is approaching on lane 2. Vehicles in lanes 1, 2, and 3 move in the opposite direction of vehicles in lanes 4, 5, and 6.

and perform collision avoidance actions in the case of assisted and autonomous driving. The kinematic information obtained from vehicle dynamics is broadcast to the communication channel, where the transmission rate of safety messages in the vehicle is controlled in real time using the congestion control approach (e.g., PULSAR [25], LIMERIC [26], reactive ETSI DCC [27], and SAE J2945/1 [18]). The information perceived by detection sensors can also be broadcast through CPMs or attached to BSMs or CAMs [22].

**C. LANE-CHANGING SCENARIO**

Lane-changing maneuvers occur on multi-lane highways that may experience different traffic conditions, e.g., one direction has free-flow traffic while in the other direction, vehicles suffer traffic congestion. In this context, it is critical to consider the combined impact of congestion control mechanisms and vehicular density on the performance of the lane-changing application. Fig. 2 visualizes a lane-changing maneuver that is influenced by the channel load generated by a varying number of communicating neighbors moving in the other direction of the highway. In this scenario, vehicle A intends to change lanes to overtake vehicle C while vehicle B is approaching A, driving on the lane intended to be occupied. The lane-changing application running on vehicle A should utilize the received safety messages for real-time tracking of the position and movement state of vehicle B to assess the feasibility of the lane-changing maneuver and avoid dangerous situations.

The lane-changing decision should determine whether a lane-changing maneuver can be performed safely based not only on local positioning and movement information but also on safety messages received from surrounding vehicles. For instance, following the representation in Fig. 2, at time instant  $t_o$ , vehicles A and C move with uniform motion at the same speed ( $v_A = v_C$ ) while maintaining a controlled distance  $D_{AC}$  between them when the first message from vehicle B is received by A.

Vehicle A would consider its lane change to be unsafe if i) vehicle B is approaching on the left lane; and ii) within

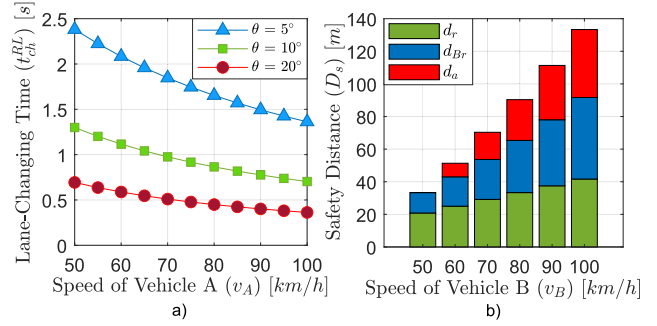


**FIGURE 3.** Safety involved parameters. a) Lane-changing time for  $\alpha_A^{ch} = 2.5 \text{ m/s}^2$  and  $l_w = 3.5 \text{ m}$  [6], [50], b) Safety distance for A and B in uniform motion with  $v_A = 50 \text{ km/h}$ ,  $t_r = 1.5 \text{ s}$  [7],  $\mu_o = 0.8$  (dry asphalt),  $t_s = 3 \text{ s}$  equivalent to  $t_{ch}^{RL} = 2.5 \text{ s}$  and  $t_m = 0.5 \text{ s}$ .

a time window ( $t_w$ ), the distance between A and B ( $d_{AB}$ ) regarding the front side of vehicles, becomes smaller than a certain safety distance ( $D_s(t)$ ) plus the length of vehicle A ( $L_A$ ), as expressed in (1).

$$d_{AB}(t) \leq D_s(t) + L_A. \tag{1}$$

The safety distance  $D_s(t)$ , presented in (2), comprises the stopping distance of vehicle B, which is the distance required by B to stop in the case of an emergency involving vehicle A, plus an additional distance ( $d_a$ ) to increase the reliability of the lane-changing maneuver.

$$D_s(t) = \overbrace{d_r + d_{Br}}^{\text{Stopping Distance of B}} + \overbrace{d_a}^{\text{Additional Distance}}. \tag{2}$$

The stopping distance in (2) includes the reaction distance ( $d_r$ ),  $d_r = v_B \cdot t_r + \frac{a_B \cdot t_r^2}{2}$ , where  $v_B$  and  $a_B$  represent B's speed and acceleration, respectively. The term  $t_r$  refers to the reaction time, which is the time required to detect a hazard and activate brakes. The stopping distance also considers the braking distance ( $d_{Br}$ ),  $d_{Br} = \frac{v_B^2 [\text{km/h}]}{250\mu_o}$  [6], which is the distance required by B to stop once the brakes have been activated, where  $\mu_o$  represents the friction coefficient of the road.

The additional distance ( $d_a$ ),  $d_a = (v_B - v_A) \cdot t_s + \frac{(a_B - a_A) \cdot t_s^2}{2}$ , depends on the relative speed of vehicles B and A, where  $a_A$  represents the acceleration of A. It also depends on the safety time ( $t_s$ ),  $t_s = t_{ch}^{RL} + t_m$ , which consists of the lane-changing time ( $t_{ch}^{RL}$ ) of vehicle A and a margin of time ( $t_m$ ) to account for potential errors in the position measurements. The lane-changing time  $t_{ch}^{RL}$ , as shown in (3), represents the time required by vehicle A to change from the right to the left lane [6],

$$t_{ch}^{RL} = \frac{-v_A + \left( v_A^2 + \frac{2a_A^{ch} l_w}{\sin \theta} \right)^{\frac{1}{2}}}{a_A^{ch}}, \quad a_A^{ch} > 0, \tag{3}$$

where  $l_w$  is lane width,  $\theta$  is the lane-changing heading, and  $a_A^{ch}$  is the lane-changing acceleration.

Fig. 3a visualizes the lane-changing time  $t_{ch}^{RL}$  on vehicle A for a typical lane-changing heading  $\theta$  ranging from  $5^\circ$  to  $20^\circ$  [51], a lane-changing acceleration  $a_A^{ch}$  of  $2.5 \text{ m/s}^2$  [6], and a common lane width  $l_w$  of  $3.5 \text{ m}$  [6], [50]. Fig. 3b illustrates the safety distance  $D_s$  according to the speed of vehicle B for an average driver's reaction time  $t_r$  of  $1.5 \text{ s}$  [7], a road friction coefficient  $\mu_o$  of  $0.8$  corresponding to dry asphalt [6], and a safety time  $t_s$  of  $3 \text{ s}$ .

### D. LANE-CHANGING APPLICATION

As specified by ETSI in [19], road safety applications should monitor the movement dynamics of target vehicles within a pre-defined time interval and decide whether to execute the maneuver or not. Accordingly, in our lane-changing test application, vehicle A employs a kinematic model and the messages received to track the position and movement state of vehicle B [6]. For each received safety message, vehicle A utilizes the position ( $P_B^{q-1}$ ), speed ( $v_B^{q-1}$ ), and acceleration ( $a_B$ ) of vehicle B to determine B's new position ( $P_B^q$ ) and speed ( $v_B^q$ ). This is accomplished by using (4), where  $q-1$  and  $q$  represent the previous and current states, respectively, and  $\Delta t$  denotes the prediction time step. If  $\Delta t$  passes without receiving a message from B, then vehicle A utilizes the previously received information to predict B's current position  $P_B^q$  and speed  $v_B^q$  [6].

$$\begin{bmatrix} P_B^q \\ v_B^q \end{bmatrix} = \begin{bmatrix} 1 & \Delta t \\ 0 & 1 \end{bmatrix} \cdot \begin{bmatrix} P_B^{q-1} \\ v_B^{q-1} \end{bmatrix} + \begin{bmatrix} \frac{\Delta t^2}{2} \\ \Delta t \end{bmatrix} a_B. \quad (4)$$

Algorithm 1 shows the steps executed by the V2V-based lane-changing application in vehicle A. Vehicles derive their position, speed, acceleration, and length from onboard sensors, e.g., from the vehicle dynamics module depicted in Fig. 1. An accurate estimation of the movement parameters can be obtained with Kalman Filters [6]. On each message received from B or state prediction, vehicle A decides whether to proceed with or abort the lane-changing maneuver, based on the estimated values of  $d_{AB}$  and  $D_s$  and the condition stated in (1). The distance  $d_{AB}$  is estimated from the positions of A ( $P_A$ ) and B ( $P_B$ ). State predictions occur at regular time intervals  $\Delta t$  after each message is received from B, and the decision to perform or abort the maneuver is taken within a time window  $t_w$ .

The lane-changing application utilizes the position, speed, and acceleration of vehicles A and B as initial conditions whereas the considered parameters are employed to estimate the safety distance and assess the condition. It is important to note that the algorithm has a main process where a function is regularly called to decide whether to abort or not the lane-changing maneuver. The main process of the algorithm starts when vehicle A receives a safety message from B. Immediately, the function is called to check the safety condition based on  $D_s$  as well as on  $d_{AB}$ . If the condition is true, the maneuver is aborted, otherwise, the position and speed of vehicle B are predicted every  $\Delta t$ . Then, the function is called again to check the safety

condition considering the new position and speed of B. This process is repeated until reaches the end of the time window or receives another safety message from vehicle B which cancels the scheduled task and starts a new main process.

### Algorithm 1 Lane-Changing Application on Vehicle A

---

**Initial Conditions:**  $\{P_A, v_A, a_A, P_B, v_B, a_B, t_o\}$   
**Considered Parameters:**  $\{t_r, t_{ch}^{RL}, t_m, L_A, \mu_o\}$   
**Result:** {ABORT}

On each safety message from B, cancel the scheduled task and do:

```

begin
1   call Decide;
2   Every  $\Delta t$  up to  $(t_o + t_w)$  do
3     Update  $\begin{bmatrix} P_B^q \\ v_B^q \end{bmatrix}$  (4);
4     call Decide;

```

**Function Decide** ( $P_B, v_B, a_B$ )

```

1   Compute  $d_{AB}$ ;
2   Compute  $D_s$  (2);
3   if  $(d_{AB} \leq D_s + L_A)$  then
4     set ABORT;

```

---

## IV. CONGESTION CONTROL

Prominent congestion control approaches based on message rate adaptation for V2V communications have been proposed [18], [25], [26], [27] to mitigate channel congestion in high-density vehicular scenarios. This work focuses on PULSAR [25], LIMERIC [26], reactive ETSI DCC [27], and SAE J2945/1 [18]. The power control and tracking error strategies in SAE J2945/1 are excluded to focus on the effect of its message rate adaptation-based congestion control mechanism on road safety.<sup>1</sup> Hence, these control methods dynamically adjust the transmission rate of safety messages to mitigate channel congestion, while maintaining a fixed vehicle power level. As specified by ETSI in [27], congestion control should have cross-layer functionality; therefore, it is not limited only to the MAC layer. Accordingly, in the proposed architecture, congestion control operates above the MAC layer controlling the transmission rate of safety messages in the vehicle (see Fig. 1).

### A. PULSAR

In PULSAR [25], the message transmission rate ( $r_{k+1}$ ) of the vehicle is computed at each iteration ( $k+1$ ) based on its previous message transmission rate ( $r_k$ ) and channel utilization ( $U_k$ ) using (5), where  $U_t$  is the target channel utilization and the parameters  $\alpha_P$  and  $\beta_P$  define the convergence behavior of the AIMD technique.

$$r_{k+1} = \begin{cases} r_k + \alpha_P, & U_k \leq U_t, \\ (1 - \beta_P)r_k, & U_k > U_t. \end{cases} \quad (5)$$

To overcome the slow convergence problem, vehicles include their current message transmission rates on BSMs or CAMs [25]. When a new message transmission rate ( $r_{new}$ ) is received, target rate ( $r_t$ ) is updated as  $r_t = (1 - \delta)r_t + \delta \cdot r_{new}$ , where  $\delta \in (0, 1)$  determines the weight of  $r_{new}$ . Then,  $r_t$  is utilized as a gravitation pull by adding the parameter  $w$  to

<sup>1</sup>The effect of all features of SAE J2945/1 on road safety will be addressed in future work.

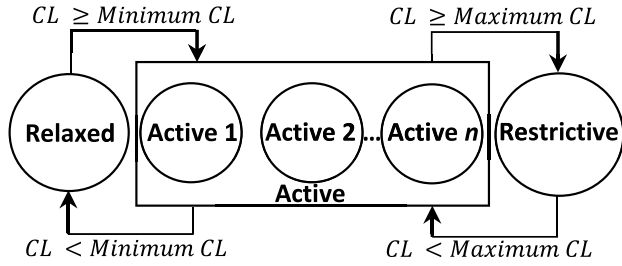


FIGURE 4. State machine on reactive ETSI DCC according to ETSI TS 102 687 [27].

the AIMD technique [25]. The parameter  $w$  is equal to the acceleration factor  $a_c$ ,  $w = a_c$ , for  $r_k \leq r_t$  or  $w = \frac{1}{a_c}$  for  $r_k > r_t$ . A higher value of  $a_c$  accelerates the convergence at the cost of decreased smoothness. PULSAR utilizes the modified AIMD with a gravitational pull, as in (6), where  $\tilde{U}_{k,2}$  is the maximum channel utilization reported for the two-hop area.

$$r_{k+1} = \begin{cases} r_k + w \cdot \alpha_P, & \tilde{U}_{k,2} \leq U_t, \\ (1 - \beta_P/w)r_k, & \tilde{U}_{k,2} > U_t. \end{cases} \quad (6)$$

### B. LIMERIC

In LIMERIC [26], vehicles adapt their message transmission rates such that channel utilization converges to a specified value. The underlying mechanism computes the message transmission rate  $\hat{r}_j(t)$  of vehicle  $j$  at time instant  $t$  according to (7), where  $\hat{r}_C(t - 1)$  is the aggregate message transmission rate of all vehicles participating in congestion control,  $\hat{r}_g$  is the goal of the total message transmission rate, and  $\alpha_L$  and  $\beta_L$  are parameters that control stability, fairness, and steady-state convergence.

$$\hat{r}_j(t) = (1 - \alpha_L)\hat{r}_j(t - 1) + \beta_L(\hat{r}_g - \hat{r}_C(t - 1)). \quad (7)$$

LIMERIC employs a gain saturation mechanism to ensure convergence in the calculation of the transmission rate of safety messages in scenarios with high vehicular density [26]. The linear rate-control equation with gain saturation is given in (8), where parameter  $X_L$  is the threshold for limiting the update offset.

$$\hat{r}_j(t) = (1 - \alpha_L)\hat{r}_j(t - 1) + \text{sign}(\hat{r}_g - \hat{r}_C(t - 1)) \cdot \min[X_L, \beta_L |\hat{r}_g - \hat{r}_C(t - 1)|]. \quad (8)$$

### C. ETSI DCC

Reactive ETSI DCC [27] employs a state machine to tackle channel congestion and provide an equitable resource division. It consists of several channel states (*relaxed*, *active*, and *restrictive*) depending on the current channel utilization, as illustrated in Fig. 4. State transitions are driven by the channel load ( $CL$ ) locally measured by each vehicle, where a higher channel utilization leads to a lower transmission rate of safety messages.

### D. SAE J2945/1

SAE J2945/1 [18] mitigates channel congestion by adapting the message transmission rate of vehicles based on the number of neighbors. Vehicles periodically estimate the number of communicating neighbors  $N(k)$  in a 100 m range at each 1000-ms interval  $k$  and compute the smoothed number of vehicles as  $N_s(k) = \lambda \cdot N(k) + (1 - \lambda) \cdot N_s(k - 1)$ , where the parameter  $\lambda_N \in (0, 1)$  is the weight factor. The vehicles then set the message transmission interval ( $T_{vITT}(k)$ ) [ms] according to (9), where  $B$  is the vehicular density coefficient, and  $T_{vMinITT}$  [ms] and  $T_{vMaxITT}$  [ms] represent the minimum and maximum allowed message transmission intervals, respectively.

$$T_{vITT}(k) = \begin{cases} T_{vMinITT}, & N_s(k) \leq B, \\ T_{vMinITT} \cdot \frac{N_s(k)}{B}, & B < N_s(k) < \frac{T_{vMaxITT}}{T_{vMinITT}} \cdot B, \\ T_{vMaxITT}, & \frac{T_{vMaxITT}}{T_{vMinITT}} \cdot B \leq N_s(k). \end{cases} \quad (9)$$

### V. INCIDENT DETECTION EVALUATION

This section introduces the simulation setup and discusses the impact of message rate adaptation-based congestion control strategies on road safety. The basic settings of the evaluation scenario and the configuration for congestion control are presented in Section V-A. The effects on the incident detection of congestion control mechanisms are discussed in Sections V-B to V-D.

#### A. CONFIGURATION

The experiments were conducted using Matlab on a straight highway with three lanes in each direction, as illustrated in Fig. 2. The lane-changing scenario is modeled in real time. In one direction of the highway, vehicles A and C move with uniform motion (i.e., with accelerations  $a_A, a_C$  of 0 m/s<sup>2</sup>) at the same speed ( $v_A = v_C$ ) maintaining a controlled distance  $D_{AC}$ , while vehicle B approaches A ( $v_B > v_A$ ) with an initial acceleration  $a_B$  of 0 m/s<sup>2</sup>. To model different lane-changing situations, speeds from 50 to 80 km/h, in steps of 10 km/h were considered for A and C. In each simulation, the speed  $v_A(v_C)$  is randomly selected from {50, 60, 70, 80} km/h.  $D_{AC}$  was defined according to the stopping distance required by vehicle A (see Section III-C). Stopping distances from 33 to 65 m are required for speeds of vehicle A between 50 and 80 km/h, considering an average driver's reaction time  $t_r$  of 1.5 s [7] and a friction coefficient  $\mu_o$  of 0.8 equivalent to dry asphalt. The initial speed of vehicle B is set with a random excess from  $v_A$  in the range of 10 to 30 km/h, in steps of 10 km/h, i.e.,  $v_B$  is  $v_A$  plus  $\text{random}\{10, 20, 30\}$  km/h.

It is defined a lane-changing acceleration  $a_A^{ch}$  for vehicle A of 2.5 m/s<sup>2</sup> and a lane width  $l_w$  equal to 3.5 m [6], [50], which for typical lane-changing headings  $\theta$  ranging from 5° to 20° [51] lead to a maximum lane-changing time  $t_{ch}^{RL}$  of 2.5 s. Accordingly, a  $t_{ch}^{RL}$  of 2.5 s (similarly to [52], [53]) and a



margin time  $t_m$  of 0.5 s were established, resulting in a safety time  $t_s$  of 3 s. The position of vehicle B is randomly selected such that, at time instant  $t_o$ , the distance  $d_{AB}$  is higher than  $D_s(t_o) + L_A$ , indicating that vehicle B is not initially a threat to vehicle A (see (1)).

To model a dangerous situation, vehicle B is programmed to accelerate within  $t_w$ , which is the time window in which A evaluates the feasibility of the lane-changing maneuver. In this scenario, an incident occurs when the distance  $d_{AB}$  becomes equal to or less than  $D_s(t) + L_A$  within  $t_w$ , as defined in (1). Note that vehicle A performs a dangerous lane change if the maneuver is not aborted. To address a wide range of incident situations, the time instant at which B accelerates is uniformly distributed within  $(t_o, t_o + t_w)$ . The acceleration of B was randomly selected from  $\{2, 2.5, 3\}$  m/s<sup>2</sup>. The maximum speed of B ( $v_B^{\max}$ ) is set to an excess of 10 km/h for  $v_B$ , resulting in a  $v_B^{\max}$  ranging from 70 to 120 km/h.

The lane-changing application is influenced by the presence of vehicles in the other direction of the highway, as illustrated in Fig. 2. As in [29], a variable number of vehicles uniformly spaced on the road were configured to achieve a vehicular density ranging from 10 to 80 veh/km/lane, in line with the vehicular densities utilized in [7]. Note that the defined vehicular densities correspond to a total of 30 to 240 veh/km, which are in the range of [24], [26], [29], leading to an approximate spacing between vehicles per lane from 100 to 12.5 m, respectively. Vehicles are equal in size and employ the IEEE 802.11p standard [10], [13]. Safety messages are broadcast following the CSMA/CA protocol with no acknowledgments, retransmissions, or multi-channel switching [6], [7], [29]. The lane-changing application runs on vehicle A as defined by Algorithm 1. A time step  $\Delta t$  of 20 ms was used for position and movement-state tracking. Vehicles A and B employ Kalman Filters to estimate their kinematic parameters. As specified in SAE J2945/1 [18], a normally distributed noise with zero mean and standard deviation of 0.3 m/s<sup>2</sup>, 0.27 m/s, and 1.5 m is used to model sensing errors. The time instants at which safety messages are received within the time window  $t_w$  are random. The transmission rates of safety messages in vehicles, including vehicle B, are controlled in real time by PULSAR [25], LIMERIC [26], reactive ETSI DCC [27], and SAE J2945/1 [18]. The lane-changing application runs on top of congestion control. Accordingly, decisions made by the application are influenced in real time by congestion control approaches. The parameter settings for the lane-changing scenario and the rate adaptation-based congestion control mechanisms are listed in Table 1.

Vehicles communicate with a fixed power level of 20 dBm at a frequency of 5.890 GHz on a shared control channel (CCH) of 10 MHz [7], [54]. Quadrature-phase-shift keying (QPSK) modulation and a code rate of 1/2 were employed, resulting in a data rate equal to 6 Mbps [13]. In line with the reasoning in [29], it is considered unity gain omnidirectional antennas as well as a constant and equal size Interference

TABLE 1. Scenario and approaches setting.

Scenario & Approaches		Parameter	Value
Operating Conditions for the Lane-Changing Application		Lanes by Direction	3
		Lane Width ( $l_w$ )	3.5 m [6], [50]
		Vehicle Length ( $L_A$ )	4 m [6]
		Vehicle Width	1.8 m [6]
		Vehicular Density	10 to 80 veh/km/lane
		Speeds of A and C at $t_o$ ( $v_A, v_C$ )	50 to 80 km/h
		Distance $D_{AC}$	33 to 65 m
		Lane-Changing Acceleration ( $\alpha_A^{ch}$ )	2.5 m/s <sup>2</sup> [6]
		Initial Speed of B ( $v_B$ )	60 to 110 km/h
		Acceleration of B	2 to 3 m/s <sup>2</sup>
		Maximum Speed of B ( $v_B^{\max}$ )	70 to 120 km/h
		Friction Coefficient ( $\mu_o$ )	0.8 (dry asphalt)
		Reaction Time ( $t_r$ )	1.5 s [7]
		Lane-Changing Time ( $t_{ch}^{RL}$ )	2.5 s
Margin Time ( $t_m$ )	0.5 s		
Safety Time ( $t_s$ )	3 s		
Prediction Interval ( $\Delta t$ )	20 ms		
Congestion Control	PULSAR [25]	$\alpha_P, \beta_P$	0.1 Hz, 0.03
		$\delta, a_c$	0.1, 2
		Target Utilization ( $U_t$ )	0.6
	LIMERIC [26]	$\alpha_L, \beta_L$	0.1, 1/150
		Goal for Total Rate ( $\hat{r}_g$ )	0.6
		Threshold ( $X_L$ )	0.0005
	SAE J2945/1 [18]	Weight Factor ( $\lambda$ )	0.05
		Density Coefficient ( $B$ )	25
		Minimum Interval ( $T_{VMiTT}$ )	100 ms
		Maximum Interval ( $T_{VMaTT}$ )	600 ms
Reactive <sup>‡</sup> ETSI DCC [27]	State	Channel Load	Message Rate
	Relaxed	< 30 %	10 Hz
	Active 1	30 % to 39 %	5 Hz
	Active 2	40 % to 49 %	2.5 Hz
	Active 3	50 % to 60 %	2 Hz
Restrictive	> 60 %	1 Hz	

<sup>†</sup> The default parameters for congestion control are used. <sup>‡</sup> Configuration for maximum transmission delay of 1 ms with transition interval of 1 s.

TABLE 2. Communication setting.

Parameter	Value
Frequency	5.890 GHz
CCH Bandwidth	10 MHz
Transmission Power	20 dBm [7]
Receiver Sensitivity	- 82 dBm [13]
Modulation	QPSK [13]
Code Rate	1/2 [13]
Data Rate	6 Mbps [13]
Antenna Height	1.5 m [54]
Dielectric Constant ( $\epsilon_r$ )	1.02 [54]
Propagation Model	Two-Ray Interference [54]

Range (IR), Carrier Sense range (CS), and Communication Range (CR). These ranges are typically assumed as fixed distances considering deterministic propagation [25], [26], [29], which is a reasonable assumption when applied to the study of congestion control. In this work, to derive IR, CS, and CR, the Two-Ray Interference Model [54] with a dielectric constant  $\epsilon_r = 1.02$  is used, which has been validated based on an extensive set of measurement campaigns on the road.<sup>2</sup> The antenna height is 1.5 m [54] and the receiver sensitivity is - 82 dBm [13], leading to an approximate IR, CS, and CR of 500 m. The communication parameters are given in Table 2.

The effect of congestion control approaches on road safety is investigated by considering the impact of message losses at the MAC and PHY levels. A message loss probability on A from 10 % to 30 % is used to model the negative impact of frame capture and multipath effects at PHY (see [55]). At the MAC layer, the probability of successful reception ( $P_S$ ) on A is modeled by utilizing the IEEE 802.11p CSMA/CA

<sup>2</sup>The Two-Ray Interference Model is included in the Vehicles in Network Simulation (Veins) framework, <https://veins.car2x.org/>.

probabilistic model presented in [29], which considers the influence of shared receivers, hidden terminals, and message sizes. Following the reasoning in [29], the shared receivers are vehicles within the CS of B, and the hidden terminals can be estimated based on the distance from B to A and the spacing between vehicles in the other direction of the highway. The time required to transmit the Preamble and Physical Layer Convergence Procedure (PLCP) header was set to 40  $\mu$ s [29].

It is worth pointing out that for evaluation purposes, this work considers BSMs or CAMs and not CPMs; however, CPMs could be included in a more advanced study to determine how much they help improve incident detection (e.g., see Fig. 2, information about B perceived by detection sensors of D could be transmitted to A). The set of experiments considered message sizes from 200 to 600 bytes [29] and time windows  $t_w$  from 1 s to 6 s [52]. Each data point shows an average of over 1,000,000 simulated incidents that occur on the road. As a performance metric, the incident detection rate (IDR) is used. The IDR is the ratio of the number of detected incidents to the total number of simulated incidents. In this study, the impact of message rate adaptation-based congestion control mechanisms on road safety is assessed under varying conditions, which are determined by different message sizes, vehicular densities, safety message losses at the PHY level, and time windows. By considering different speeds, stopping distances, accelerations, and onboard sensor errors, diverse lane-changing situations are modeled providing valuable insights into the performance of the application. In the following, the discussion focuses on the mean values of the message rate, channel load,  $P_s$ , and IDR, as these address the action of congestion control and show the road safety perspective.

**B. ANALYZING THE EFFECT OF MESSAGE SIZE**

Fig. 5 shows the influence of congestion control mechanisms on key performance parameters for road safety depending on message size utilizing a vehicular density of 70 veh/km/lane. A high density is used because congestion control effects are more significant for a large number of vehicles, and the focus is on analyzing the joint influence of message size and vehicular density on the capability of the lane-changing application to detect unsafe maneuvers. As specified by ETSI in [17], the transmission rate of safety messages is constrained from 1 Hz to 10 Hz. The incident detection rate of the lane-changing test application on vehicle A depends on the message rate of B, reception probability in A, and time window  $t_w$ . Accordingly, Fig. 5a shows the transmission rate of safety messages in B, Fig. 5b shows the normalized channel load computed by the congestion control mechanisms, Fig. 5c shows the achieved values of  $P_s$  on A, and Fig. 5d visualizes the IDR on A for a  $t_w$  of 2 s and a message loss probability on the channel of 20 %. A time window  $t_w$  of 2 s is used because in the lane-changing application, receiving at least one timely safety message is sufficient to cancel the maneuver,

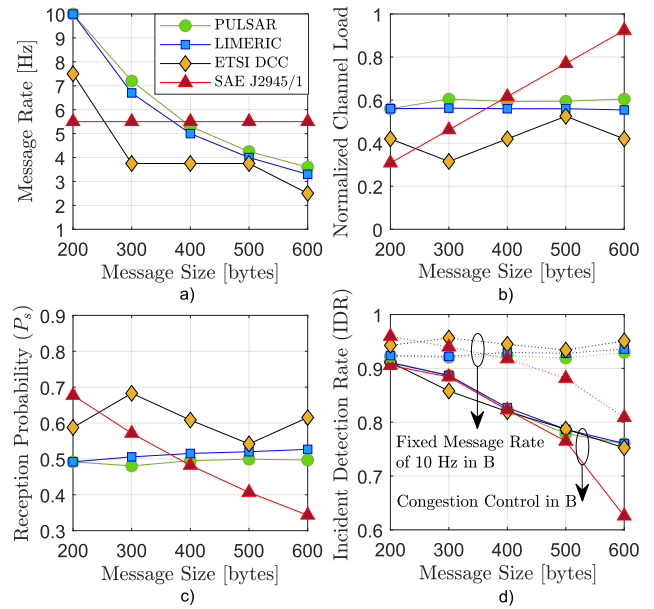


**FIGURE 5.** Performance according to the message size for a vehicular density of 70 veh/km/lane. Configuration for d)  $t_w$  of 2 s and loss probability at PHY of 20 %.

and a higher  $t_w$  neglects the effect of congestion control mechanisms.

Fig. 5a and Fig. 5d show that an increase in message size not only leads to a lower transmission rate of safety messages in B for PULSAR [25], LIMERIC [26], and reactive ETSI DCC [27], but also to a lower IDR in A for all control mechanisms when vehicle B is involved in congestion control, implying a potential risk for road safety. Fig. 5a demonstrates the effectiveness of PULSAR and LIMERIC in providing equitable resource division and ensuring fairness in the rate allocation of safety messages. Although PULSAR and LIMERIC employ different underlying control mechanisms, specifically AIMD with gravitational pull and linear rate-control with gain saturation, respectively, both strategies yield similar average message rates in vehicles with an increase in the size of the safety messages. This is because both methods equitably distribute the available communication resources among vehicles to maintain the channel utilization below 60% of the channel capacity, as observed in Fig. 5b and Table 1.

The reactive ETSI DCC [27] also provides equitable resource division; however, unlike PULSAR and LIMERIC, it utilizes a state machine with different levels of channel utilization, as shown in Fig. 4 and Table 1. The underlying mechanism of this approach suffers from unstable state transitions, which causes oscillations in the transmission rates of safety messages assigned to vehicles [7]. Consequently, the message rate in B oscillates between 10 Hz and 5 Hz for a message size of 200 bytes, between 5 Hz and 2.5 Hz for a message size from 300 to 500 bytes, while remaining stable in 2.5 Hz for a message size of 600 bytes. Fig. 5a shows that an increase in message size also leads to a reduction in

the average message rates of B with the reactive ETSI DCC. Fig. 5b visualizes that the oscillatory nature of this approach is also reflected in the channel load, which can effectively mitigate channel congestion.

On the other hand, SAE J2945/1 [18] computes, in this traffic setup, approximately 45 communicating vehicles in a range of 100 m, leading to a message transmission interval of 180 ms equivalent to a message transmission rate in vehicle B of 5.5 Hz, as observed in Fig. 5a. Because the message rate is adapted based solely on the number of surrounding vehicles, it is not affected by the message size. However, an increase in message size also leads to a higher channel load (see Fig. 5b), resulting in a lower probability of successful reception of safety messages in A due to packet collisions, as shown in Fig. 5c. This issue indicates the necessity of using a power control strategy in SAE J2945/1, but the adaptation of transmission power based solely on channel load can lead to harmful warning distances, imposing a challenge for road safety because vehicles need to be notified at a sufficient distance from the expected impact to take collision-avoidance actions [7], [19].

Importantly, Fig. 5b and Fig. 5c show that the channel load is directly related to the probability of successful reception  $P_s$  of safety messages in A. Specifically, an increase in channel utilization degrades  $P_s$ , impairing the capability of the lane-changing application to detect unsafe maneuvers. In particular, when the message size increases from 300 to 500 bytes,  $P_s$  in A decreases from almost 70 % to 55 % for reactive ETSI DCC, despite the message rate in B remaining constant at 3.75 Hz. This also occurs for SAE J2945/1, where an increase in the size of messages from 200 to 600 bytes degrades  $P_s$  from almost 70 % to 35 % although B's message rate is fixed at 5.5 Hz, leading to an IDR of 62 % on A for a message size of 600 bytes (see Fig. 5d). An increase in the probability of packet collisions is responsible for this phenomenon.

It is observed that the intrinsic operation of the addressed congestion control mechanisms leads to a dependency between B's message rate and A's probability of successful reception  $P_s$  which may limit road safety. For instance, the smaller the message size, the greater the transmission rate of safety messages in vehicle B, which is convenient for detecting an incident. However, such message size reduction simultaneously increases the message rates of the remaining vehicles, leading to a higher interference in vehicle A, and hence to a lower  $P_s$  and IDR. Further, it is important to highlight that the underlying congestion control mechanisms do not take into account specific vehicle dynamics which also affects road safety since B is incapable of guaranteeing a high message rate when it changes its movement state. These drawbacks are responsible for all congestion control approaches exhibiting similar incident detection downtrends, as shown in Fig. 5d.

To demonstrate the effect of congestion control on road safety, Fig. 5d visualizes the IDR on vehicle A when vehicle B participates in congestion control in comparison

with the case in which B utilizes a fixed message rate of 10 Hz. As observed, the IDR on A may drop from 90 % to less than 80 % if the message size increases from 200 to 600 bytes and the message rate of B is controlled by congestion control. Furthermore, the influence of congestion control on the incident detection rate of the lane-changing application is more significant than that of a fixed message rate of 10 Hz for a higher message size. Note that the IDR on vehicle A is reduced by at least 15 % for a message size of 600 bytes with congestion control, highlighting the importance of using a high transmission rate for safety messages in B according to its movement state.

### C. ANALYZING THE EFFECT OF VEHICULAR DENSITY

Fig. 6 shows that vehicular density, in conjunction with rate adaptation-based congestion control, may also influence the incident detection rate at the application level. In this case, the key performance parameters for road safety are shown for a message size of 378 bytes [7], [26], whereas the IDR of vehicle A is visualized in Fig. 6d for a  $t_w$  of 2 s and a PHY layer message loss probability of 20 %. Fig. 6a shows that the underlying congestion control mechanisms lead vehicle B to reduce the transmission rate of safety messages when the vehicular density in the opposite direction of the highway is increased. This negatively affects the capability of the lane-changing application on vehicle A to detect unsafe lane-changing maneuvers because B's movement state is not considered in the message rate adaptation, as shown in Fig. 6d. Fig. 6a shows that increased vehicular densities in PULSAR [25] and LIMERIC [26] led to a more efficient distribution of available channel resources than the classification mechanism employed by the reactive ETSI DCC [27]. Fig. 6b also evidences that PULSAR and LIMERIC are capable of successfully limiting channel utilization to 60% in dense scenarios.

In these traffic situations, the transmission rate of safety messages computed by B with reactive ETSI DCC remains stable in 10 Hz for a vehicular density of 10 veh/km/lane, oscillates between 10 Hz and 5 Hz for a density ranging from 20 to 30 veh/km/lane, remains stable in 5 Hz for a density ranging from 40 to 50 veh/km/lane, and oscillates between 5 Hz and 2.5 Hz for a density ranging from 60 to 80 veh/km/lane, resulting in a reduced average message rate, as observed in Fig. 6a. Fig. 6b shows that similar to the message size case, the reactive ETSI DCC can also effectively regulate channel utilization according to vehicular density. In SAE J2945/1 [18], the number of communicating neighbors within a range of 100 m increases from approximately 9 to 51 vehicles for a vehicular density of 10 to 80 veh/km/lane, respectively. Consequently, the message transmission interval in B increases from 100 ms to 204 ms, equivalent to a reduction in the message rate from 10 Hz to 4.9 Hz,

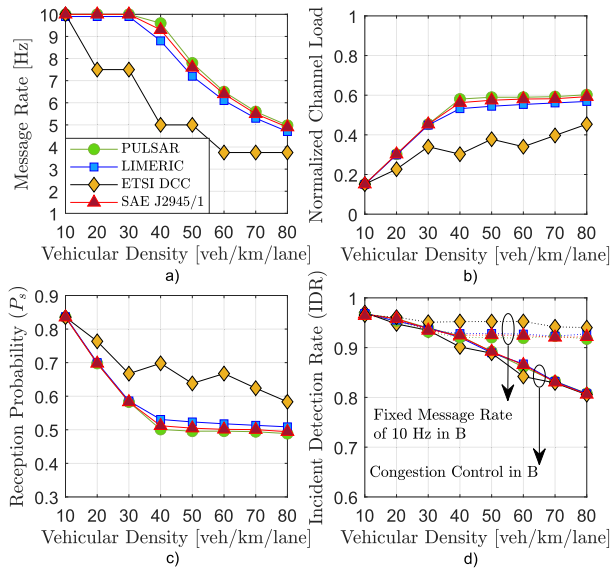


**FIGURE 6.** Performance according to the vehicular density for a message size of 378 bytes. Configuration for d)  $t_w$  of 2 s and loss probability at PHY of 20 %.

showing similar behavior to PULSAR and LIMERIC (see Fig. 6a and Fig. 6b).

Fig. 6c visualizes that an increase in vehicular density leads to a degradation in the probability of successful reception  $P_s$  of safety messages on A due to an increase in channel load, and hence, to a lower IDR when the message rate of B is adapted by congestion control, see Fig. 6d. This evidences that the incident is less likely to be detected if the interference generated by vehicles in the congested section of the road is increased. Further, in all congestion control mechanisms, a change in vehicular density may limit road safety. For instance, the gain in message rate due to a reduction of the vehicular density could limit the gain in the IDR since the higher message rate leads to higher interference [29]. In this sense, Fig. 6d shows that the IDR on A may drop from 98 % to 80 % when the vehicular density increases from 10 to 80 veh/km/lane and B operates with congestion control. Furthermore, the IDR on vehicle A is impaired by at least 10 % due to congestion control mechanisms in comparison with the case when vehicle B utilizes a fixed message transmission rate of 10 Hz for a vehicular density higher than 70 veh/km/lane.

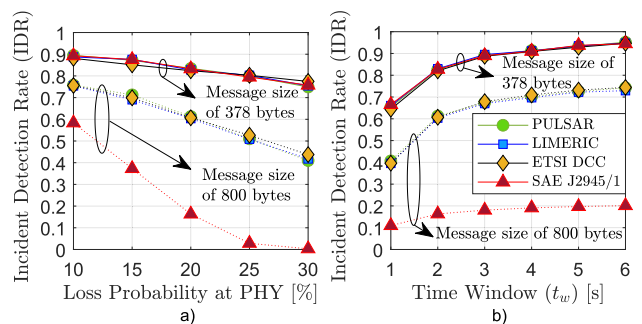
#### D. INFLUENCE OF LOSSES AT PHY LAYER AND THE TIME WINDOW

Fig. 7 evidences the influence of message loss probability at PHY and time window  $t_w$  on the incident detection rate in the presence of congestion control for a message size of 378 bytes and a vehicular density of 70 veh/km/lane. Fig. 7a visualizes the IDR on A for a  $t_w$  of 2 s, whereas a message loss probability at PHY of 20 % is utilized in Fig. 7b. As specified in [8] and [56], enhanced V2X services for platooning, extended sensors, and advanced driving with

a high level of automation may require a message size higher than 600 bytes, imposing an additional challenge for road safety. Consequently, in Fig. 7, the analysis is extended to a message size of 800 bytes. As expected, frame capture and multipath effects impair the decision-making of the lane-changing application on A, which is more critical when a higher message size is required, see Fig. 7a, and the feasibility of the maneuver is evaluated in a shorter  $t_w$ , as observed in Fig. 7b.

Fig. 7a shows that an increase from 10 % to 30 % in the message loss probability at PHY reduces the IDR on A by approximately 12 % in all congestion control approaches for a message size of 378 bytes. If a message size of 800 bytes is employed, the IDR on A drops from approximately 75 % to less than 50 % for PULSAR, LIMERIC, and ETSI DCC. This increase in message size also significantly affects the incident detection capability of the lane-changing application with SAE J2945/1, reducing the IDR on A from almost 60 % to less than 10 % for a message loss probability at the PHY layer higher than 25 %. This is because a message size of 800 bytes critically increases the channel load with SAE J2945/1, leading to a drastic reduction in the reception probability, as shown in Fig. 7b.

Fig. 7b also shows that a  $t_w$  of 1 s significantly reduces the capability of detecting unsafe maneuvers on A. However, a  $t_w$  of 6 s improves the IDR reducing the effect that congestion control mechanisms, message size, and vehicular density may have on the IDR because it increases the probability of receiving at least one safety message on vehicle A after B has changed its movement state. However, a longer  $t_w$  will increase the waiting time in A to make a decision, which may lead to missing the opportunity to execute the lane-changing maneuver. Hence,  $t_w$  requires careful tuning and further investigation. Finally, supporting more demanding safety services for assisted and autonomous driving with strict operational requirements poses an additional challenge for tuning  $t_w$ . Fig. 7b shows that for a message size of 378 bytes and a  $t_w$  from 2 s to 4 s, the IDR on A increases from 82 % to 91 %. However, if the message size is 800 bytes, the best-case IDR on A does not surpass 62 % for a  $t_w$  of 2 s and 72 % for a  $t_w$  of 4 s, irrespective of the congestion control mechanism employed.



**FIGURE 7.** Incident detection rate for vehicular density of 70 veh/km/lane with a)  $t_w$  of 2 s, b) Loss probability at PHY of 20 %.

## VI. OVERALL FINDINGS AND RECOMMENDATIONS

The evaluation results show that road incident detection rates may drop from over 90 % to less than 50 % depending on the operating conditions. Parameters such as message size, vehicular density, losses at the physical layer, and observation time of the road safety application may significantly influence the capability to detect unsafe maneuvers effectively under message rate adaptation-based congestion control. The intrinsic operation of the addressed congestion control techniques, in conjunction with the fact that vehicle dynamics are not considered, leads to a dependency between the message transmission rate and the reception probability in target vehicles, which may limit incident detection rates, especially when a high number of vehicles and larger message sizes are involved.

PULSAR and LIMERIC are effective in equitably distributing available communication resources, ensuring not only fairness in the message rate allocation but also limiting the channel load to a pre-defined threshold. However, at the same time, their underlying control mechanisms can lead to a reduced message rate in vehicles involved in lane-changing, which implies a potential risk to road safety. Conversely, the underlying control mechanism based on the state machine of a reactive ETSI DCC is able to regulate the channel load. However, it can cause undesirable oscillations and may result in an inadequate message rate. SAE J2945/1 is also capable of reducing channel congestion; however, because the message rate is adapted based on the number of neighbors, it also leads to a higher channel utilization and a lower probability of successful reception owing to packet collisions with an increase in message size.

The evaluation results also demonstrate that the channel load is directly related to the probability of successful reception in the vehicle performing lane-changing and, hence, to decision-making at the application level. Further, frame capture and multipath effects, as well as the observation time window, significantly influence the performance of the safety application. A lower time window decreases the incident detection rate, whereas increasing the time window improves the probability of detecting the incident but may also lead to losing the opportunity to execute the maneuver. Furthermore, controlling channel congestion presents a significant challenge when factoring in the operational needs of enhanced V2X services. These services, which provide a high level of automation, are fundamental for assisted and autonomous driving.

Based on the evaluation results, specific recommendations and guidelines for congestion control are provided to improve the incident detection capability of road safety applications. First, more in-depth research in the design and configuration of rate adaptation-based congestion control is required. This research should include the background effects of the congestion control mechanism on the transmission rate of safety messages. Additionally, it should consider the probability of successful reception in the targeted vehicles. Both of these

factors are crucial for the application-level performance of incident detection. In this sense, it is essential to integrate vehicle dynamics into the intrinsic operation of congestion control techniques. A message transmission rate according to the vehicle dynamics not only increases the probability of timely communication changes in the motion state of vehicles moving at high speeds but may also reduce interference from neighbors.

Second, congestion control needs to factor in its potential influence on the application's decisions and how this meets the operational requirements of highly demanding services in assisted and autonomous driving. This involves not only the size of the messages but also their frequency. Achieving a balance is key to successfully supporting enhanced V2X services in emerging technologies, such as IEEE 802.11bd and 5G NR V2X. Third, the impact of message rate adaptation-based congestion control on road safety can be minimized by designing cooperative safety applications in which vehicles work together to identify an incident. However, the design of cooperative applications is a complex task that remains an open challenge.

## VII. CONCLUSION AND FUTURE WORK

This paper studied the influence of message rate adaptation-based congestion control from the road safety perspective, focusing on the decision-making process required by road safety applications. Specifically, it was examined how prominent approaches for congestion control, such as PULSAR, LIMERIC, reactive ETSI DCC, and SAE J2945/1, impact the capability of a lane-changing application, which relies on vehicle-to-vehicle communications to detect unsafe maneuvers under varying conditions. The comparative evaluation demonstrated that congestion control, in conjunction with message size, vehicular density, message loss probability at the physical level, and the decision time window, can significantly influence the incident detection rates achieved by the safety application. It was also observed that the underlying control mechanisms led to a dependency between message transmission rate and reception probability in targeted vehicles, which limited road safety decisions. The challenges will be exacerbated by the highly demanding operational requirements defined for critical safety services in assisted and autonomous driving.

The proposed model can be extended in various aspects. It is worth pointing out that intelligent operation modes where vehicles cooperate to avoid an accident do not allow evidencing the influence of congestion control on the performance of the lane-changing application. While the model considers a straight road, it is acknowledged its potential for extension to more complex road scenarios by including the vehicle heading in the operation mode of the lane-changing application. Moreover, the model focuses on the IEEE 802.11p standard, but it could be extended to consider vehicular technologies such as IEEE 802.11bd and C-V2X (LTE V2X and 5G NR V2X). However,

the derivation of the probability of successful reception based on relevant parameters for congestion control as well as the design and evaluation of congestion control mechanisms for these recent technologies remain an open challenge.

In the model, a larger safety distance was set for a higher speed, which is a reasonable assumption from a road safety viewpoint, but other approaches are also possible to define the safety distance (e.g., fixed). The work focused on studying the effect of message rate adaptation due to the significance of this dimension within the standardized congestion control methods, and because the adaptation of transmission power or data rate poses a challenge to isolate the effect that underlying congestion control mechanisms may have on the performance of the road safety application. Given the focus of the research and to demonstrate the impact of message rate adaptation-based congestion control, this study exclusively considered safety messages. However, it could also be extended to evaluate the influence of Collective Perception Messages, which will be included in future works to explore how the data gathered by detection sensors contributes to enhancing the incident detection capabilities of road safety applications.

Future work will be oriented to extend the proposed model by adapting and examining the congestion control methods within the evolving vehicular technologies IEEE 802.11bd and 5G NR V2X. These platforms anticipate enabling more sophisticated road safety services. Additionally, the aim is to design strategies focused on road safety-oriented congestion control. This takes into account the potential advantages of incorporating collaborative applications to enhance incident detection. Future work also aims to extend the study to other relevant vehicular scenarios and road safety applications as well as consider practical tests to increase the impact of the findings.

## REFERENCES

- [1] N. H. Hussein, C. T. Yaw, S. P. Koh, S. K. Tiong, and K. H. Chong, "A comprehensive survey on vehicular networking: Communications, applications, challenges, and upcoming research directions," *IEEE Access*, vol. 10, pp. 86127–86180, 2022.
- [2] S. V. Balkus, H. Wang, B. D. Cornet, C. Mahabal, H. Ngo, and H. Fang, "A survey of collaborative machine learning using 5G vehicular communications," *IEEE Commun. Surveys Tuts.*, vol. 24, no. 2, pp. 1280–1303, 2nd Quart., 2022.
- [3] Y. Fu, C. Li, F. R. Yu, T. H. Luan, and Y. Zhang, "A survey of driving safety with sensing, vehicular communications, and artificial intelligence-based collision avoidance," *IEEE Trans. Intell. Transp. Syst.*, vol. 23, no. 7, pp. 6142–6163, Jul. 2022.
- [4] J. Wang, J. Liu, and N. Kato, "Networking and communications in autonomous driving: A survey," *IEEE Commun. Surveys Tuts.*, vol. 21, no. 2, pp. 1243–1274, 2nd Quart., 2019.
- [5] G. Thandavarayan, M. Sepulcre, and J. Gozalvez, "Cooperative perception for connected and automated vehicles: Evaluation and impact of congestion control," *IEEE Access*, vol. 8, pp. 197665–197683, 2020.
- [6] S. Bolufé, C. A. Azurdia-Meza, S. Céspedes, and S. Montejo-Sánchez, "Impact of awareness control on V2V-based overtaking application in autonomous driving," *IEEE Commun. Lett.*, vol. 25, no. 4, pp. 1373–1377, Apr. 2021.
- [7] S. Bolufé, C. A. Azurdia-Meza, S. Céspedes, S. Montejo-Sánchez, R. D. Souza, and E. M. G. Fernandez, "POSACC: Position-accuracy based adaptive beaconing algorithm for cooperative vehicular safety systems," *IEEE Access*, vol. 8, pp. 15484–15501, 2020.
- [8] M. H. C. Garcia, A. Molina-Galan, M. Boban, J. Gozalvez, B. Coll-Perales, T. Sahin, and A. Kousaridas, "A tutorial on 5G NR V2X communications," *IEEE Commun. Surveys Tuts.*, vol. 23, no. 3, pp. 1972–2026, 3rd Quart., 2021.
- [9] B. Häfner, V. Bajpai, J. Ott, and G. A. Schmitt, "A survey on cooperative architectures and maneuvers for connected and automated vehicles," *IEEE Commun. Surveys Tuts.*, vol. 24, no. 1, pp. 380–403, 1st Quart., 2022.
- [10] F. Arena, G. Pau, and A. Severino, "A review on IEEE 802.11p for intelligent transportation systems," *J. Sensor Actuator Netw.*, vol. 9, no. 2, p. 22, 2020.
- [11] *Part 11: Wireless LAN Medium Access Control (MAC) and Physical Layer (PHY) Specifications—Amendment 5: Enhancements for Next Generation V2X*, IEEE Standard 802.11bd, 2022.
- [12] M. M. Saad, M. T. R. Khan, S. H. A. Shah, and D. Kim, "Advancements in vehicular communication technologies: C-V2X and NR-V2X comparison," *IEEE Commun. Mag.*, vol. 59, no. 8, pp. 107–113, Aug. 2021.
- [13] *Part 11: Wireless LAN Medium Access Control (MAC) and Physical Layer (PHY) Specifications*, IEEE Standard 802.11-2016, 2020.
- [14] S. Zeadally, M. A. Javed, and E. B. Hamida, "Vehicular communications for ITS: Standardization and challenges," *IEEE Commun. Standards Mag.*, vol. 4, no. 1, pp. 11–17, Mar. 2020.
- [15] S. A. Yusuf, A. Khan, and R. Souissi, "Vehicle-to-everything (V2X) in the autonomous vehicles domain—A technical review of communication, sensor, and AI technologies for road user safety," *Transp. Res. Interdiscipl. Perspect.*, vol. 23, pp. 1–23, Jan. 2024.
- [16] *Vehicle-to-Everything (V2X) Communications Message Set Dictionary*, Standard SAE J2735, 2022.
- [17] *Intelligent Transport Systems (ITS); Vehicular Communications; Basic Set of Applications; Part 2: Specification of Cooperative Awareness Basic Service*, Standard ETSI EN 302 637-2, Version 1.4.1, 2019.
- [18] *On-Board System Requirements for V2V Safety Communications*, Standard SAE J2945/1, 2020.
- [19] *Intelligent Transport Systems (ITS); V2X Applications; Part 3: Longitudinal Collision Risk Warning (LCRW) Application Requirements Specification*, Standard ETSI TS 101 539-3 V1.1.1, 2013.
- [20] M. S. Sheikh and Y. Peng, "Improved collision risk assessment for autonomous vehicles at on-ramp merging areas," *IEEE Access*, vol. 11, pp. 130974–130989, 2023.
- [21] M. S. Sheikh and Y. Peng, "Modeling collision risk for unsafe lane-changing behavior: A lane-changing risk index approach," *Alexandria Eng. J.*, vol. 88, pp. 164–181, Feb. 2024.
- [22] *Intelligent Transport Systems (ITS); Vehicular Communications; Basic Set of Applications; Analysis of the Collective Perception Service (CPS)*, Standard ETSI TR 103 562 V2.1.1, 2019.
- [23] A. D. S. Roque, N. Jazdi, E. P. De Freitas, and C. E. Pereira, "A fault modeling based runtime diagnostic mechanism for vehicular distributed control systems," *IEEE Trans. Intell. Transp. Syst.*, vol. 23, no. 7, pp. 7220–7232, Jul. 2022.
- [24] T. Shimizu, B. Cheng, H. Lu, and J. Kenney, "Comparative analysis of DSRC and LTE-V2X PC5 mode 4 with SAE congestion control," in *Proc. IEEE Veh. Netw. Conf. (VNC)*, Dec. 2020, pp. 1–8.
- [25] T. Tielert, D. Jiang, Q. Chen, L. Delgrossi, and H. Hartenstein, "Design methodology and evaluation of rate adaptation based congestion control for vehicle safety communications," in *Proc. IEEE Veh. Netw. Conf. (VNC)*, Nov. 2011, pp. 116–123.
- [26] G. Bansal, J. B. Kenney, and C. E. Rohrs, "LIMERIC: A linear adaptive message rate algorithm for DSRC congestion control," *IEEE Trans. Veh. Technol.*, vol. 62, no. 9, pp. 4182–4197, Nov. 2013.
- [27] *Intelligent Transport Systems (ITS); Decentralized Congestion Control Mechanisms for Intelligent Transport Systems Operating in the 5 GHz Range; Access Layer Part*, Standard ETSI TS 102 687 V1.2.1, 2018.
- [28] B. Shabir, M. A. Khan, A. U. Rahman, A. W. Malik, and A. Wahid, "Congestion avoidance in vehicular networks: A contemporary survey," *IEEE Access*, vol. 7, pp. 173196–173215, 2019.
- [29] M. Van Eenennaam, W. K. Wolterink, G. Karagiannis, and G. Heijenk, "Exploring the solution space of beaconing in VANETs," in *Proc. IEEE Veh. Netw. Conf. (VNC)*, Oct. 2009, pp. 1–8.

- [30] T. Lorenzen and M. T. Garrosi, "Achieving global fairness at urban intersections using cooperative DSRC congestion control," in *Proc. 1st ACM Int. Workshop Smart, Auto., Connected Veh. Syst. Services*, Oct. 2016, pp. 52–59.
- [31] C. Campolo, A. Molinaro, and R. Scopigno, *Vehicular Ad Hoc Networks: Standards, Solutions, and Research*. Springer, 2015.
- [32] A. Autolitano, C. Campolo, A. Molinaro, R. M. Scopigno, and A. Vesco, "An insight into decentralized congestion control techniques for VANETs from ETSI TS 102 687 V1.1.1," in *Proc. IFIP Wireless Days (WD)*, Nov. 2013, pp. 1–6.
- [33] S. Kühlmorgen, H. Lu, A. Festag, J. Kenney, S. Gensheim, and G. Fettweis, "Evaluation of congestion-enabled forwarding with mixed data traffic in vehicular communications," *IEEE Trans. Intell. Transp. Syst.*, vol. 21, no. 1, pp. 233–247, Jan. 2020.
- [34] J. Aznar-Poveda, E. Egea-Lopez, A.-J. Garcia-Sanchez, and P. Pavon-Mariño, "Time-to-collision-based awareness and congestion control for vehicular communications," *IEEE Access*, vol. 7, pp. 154192–154208, 2019.
- [35] I. Soto, O. Amador, M. Urueña, and M. Calderon, "Strengths and weaknesses of the ETSI adaptive DCC algorithm: A proposal for improvement," *IEEE Commun. Lett.*, vol. 23, no. 5, pp. 802–805, May 2019.
- [36] O. Amador, I. Soto, M. Calderón, and M. Urueña, "Experimental evaluation of the ETSI DCC adaptive approach and related algorithms," *IEEE Access*, vol. 8, pp. 49798–49811, 2020.
- [37] M. Karoui, G. Chalhoub, and A. Freitas, "A study of congestion control approaches for vehicular communications using ITS-G5," in *Proc. IEEE 31st Annu. Int. Symp. Pers., Indoor Mobile Radio Commun.*, Aug. 2020, pp. 1–7.
- [38] A. Balador, E. Cinque, M. Pratesi, F. Valentini, C. Bai, A. A. Gómez, and M. Mohammadi, "Survey on decentralized congestion control methods for vehicular communication," *Veh. Commun.*, vol. 33, Jan. 2022, Art. no. 100394.
- [39] N. Mohammed and R. A. Kadhim, "Congestion control in VANETs based on message rate adaptation by the exponential function," in *Proc. 5th Int. Seminar Res. Inf. Technol. Intell. Syst. (ISRITI)*, Dec. 2022, pp. 24–28.
- [40] A. Ibrahim, D. Goswami, H. Li, and T. Basten, "Delay-aware multi-layer multi-rate model predictive control for vehicle platooning under message-rate congestion control," *IEEE Access*, vol. 10, pp. 44583–44607, 2022.
- [41] M. I. Khan, J. Härrä, and S. Sesia, "Enhancing ETSI DCC for multi-service vehicular safety communication," in *Proc. IEEE 92nd Veh. Technol. Conf. (VTC-Fall)*, Nov. 2020, pp. 1–5.
- [42] B. Toghi, M. Saifuddin, Y. P. Fallah, and M. O. Mughal, "Analysis of distributed congestion control in cellular vehicle-to-everything networks," in *Proc. IEEE 90th Veh. Technol. Conf. (VTC-Fall)*, Sep. 2019, pp. 1–7.
- [43] Y. Yoon and H. Kim, "Balancing power and rate control for improved congestion control in cellular V2X communication environments," *IEEE Access*, vol. 8, pp. 105071–105081, 2020.
- [44] K. Takahashi and S. Shioda, "Distributed congestion control method for sending safety messages to vehicles at a set target distance," *Ann. Telecommun.*, vol. 79, nos. 3–4, pp. 211–225, Apr. 2024.
- [45] E. Egea-Lopez, P. Pavon-Mariño, and J. Santa, "Optimal joint power and rate adaptation for awareness and congestion control in vehicular networks," *IEEE Trans. Intell. Transp. Syst.*, vol. 23, no. 12, pp. 25033–25046, Dec. 2022.
- [46] Y. Fang, X. Liu, Z. Li, L. Cui, K. Wei, and Q. Deng, "Efficient congestion control with information loss minimization for vehicular Ad hoc networks," *IEEE Trans. Veh. Technol.*, vol. 72, no. 3, pp. 3879–3888, Mar. 2023.
- [47] L. K. Ouladdjedid, C. T. Calafate, C. A. Kerrache, and Y. Guellouma, "Analysis of congestion control mechanisms for cooperative awareness in IoV environments," *Electronics*, vol. 12, no. 3, p. 512, Jan. 2023.
- [48] T. K. Mishra, K. S. Sahoo, M. Bilal, S. C. Shah, and M. K. Mishra, "Adaptive congestion control mechanism to enhance TCP performance in cooperative IoV," *IEEE Access*, vol. 11, pp. 9000–9013, 2023.
- [49] J. M. I. Parella, O. T. Ajayi, and Y. Cheng, "Adaptive messaging based on the age of information in VANETs," in *Proc. IEEE Global Commun. Conf. (GLOBECOM)*, Dec. 2022, pp. 1235–1240.
- [50] O. Popescu, S. Sha-Mohammad, H. Abdel-Wahab, D. C. Popescu, and S. El-Tawab, "Automatic incident detection in intelligent transportation systems using aggregation of traffic parameters collected through V2I communications," *IEEE Intell. Transp. Syst. Mag.*, vol. 9, no. 2, pp. 64–75, Apr. 2017.
- [51] Q. Yang, F. Lu, J. Wang, D. Zhao, and L. Yu, "Analysis of the insertion angle of lane-changing vehicles in nearly saturated fast road segments," *Sustainability*, vol. 12, no. 3, p. 1013, Jan. 2020.
- [52] M. Sepulcre and J. Gozalvez, "On the importance of application requirements in cooperative vehicular communications," in *Proc. 8th Int. Conf. Wireless On-Demand Netw. Syst. Services*, Jan. 2011, pp. 124–131.
- [53] M. Sepulcre and J. Gozalvez, "Experimental evaluation of cooperative active safety applications based on V2V communications," in *Proc. 9th ACM Int. Workshop Veh. Inter-Netw., Syst., Appl.*, Jun. 2012, pp. 13–20.
- [54] C. Sommer, S. Joerer, and F. Dressler, "On the applicability of two-ray path loss models for vehicular network simulation," in *Proc. IEEE Veh. Netw. Conf. (VNC)*, Nov. 2012, pp. 64–69.
- [55] M. Sepulcre, M. Gonzalez-Martín, J. Gozalvez, R. Molina-Masegosa, and B. Coll-Perales, "Analytical models of the performance of IEEE 802.11p vehicle to vehicle communications," *IEEE Trans. Veh. Technol.*, vol. 71, no. 1, pp. 713–724, Jan. 2022.
- [56] *Enhancement of 3GPP Support for V2X Scenarios (Release 17)*, document 3GPP TS 22.186, Version 17.0.0, 2022.



**SANDY BOLUFÉ** (Member, IEEE) received the B.Sc. degree in electronics and telecommunications engineering and the M.Sc. degree in telematics from the Central University of Las Villas (UCLV), Santa Clara, Cuba, in 2009 and 2016, respectively, and the Ph.D. degree in electrical engineering from Universidad de Chile, Santiago, Chile, in 2021. He is currently an Assistant Professor with the Department of Electrical Engineering, University of Santiago of Chile (USACH), Santiago, Chile. His research interests include vehicular communications systems, autonomous driving, 5G and beyond enabling technologies, and the Internet of Things. He was a co-recipient of the 2021 11th Abertis International Award in Road Safety. He has served as a Reviewer for IEEE Vehicular Technology Magazine, IEEE Access, IET Communications, IEEE LATINCOM, and IEEE Vehicular Networking Conference.



**JORGE F. SILVA** (Senior Member, IEEE) received the M.Sc. and Ph.D. degrees in electrical engineering from the University of Southern California (USC), Los Angeles, CA, USA, in 2005 and 2008, respectively. From 2003 to 2008, he was a Research Assistant with the Signal Analysis and Interpretation Laboratory (SAIL), USC. He was also a Research Intern with the Speech Research Group, Microsoft Corporation, Redmond, WA, USA, in 2005. He is currently an Associate

Professor with the Department of Electrical Engineering (EE), University of Chile, and a Principal Investigator with the Advanced Center of Electrical and Electronic Engineering, Valparaíso, Chile. He received the Outstanding Thesis Award for Theoretical Research of the Viterbi School of Engineering, in 2009, the Viterbi Doctoral Fellowship, from 2007 to 2008, and the Simon Ramo Scholarship at USC, from 2007 to 2008. He was an Associate Editor of IEEE TRANSACTIONS ON SIGNAL PROCESSING, from 2016 to 2018.



**CESAR A. AZURDIA-MEZA** (Member, IEEE) received the B.Sc. degree in electrical engineering from the Universidad del Valle de Guatemala, Guatemala, in 2005, the M.Sc. degree in electrical engineering from Linnaeus University, Sweden, in 2009, and the Ph.D. degree in electronics and radio engineering from Kyung Hee University, Republic of South Korea, in 2013. In August 2013, he joined the Department of Electrical Engineering, University of Chile, as an Assistant

Professor, where he is currently an Associate Professor, lecturing on wireless and mobile communication systems. He has been a Principal Investigator of several national and international research grants. His research interests include Nyquist's ISI criterion, OFDM-based systems, SC-FDMA, visible light communication systems, vehicular communications, 5G and beyond enabling technologies, and signal processing techniques for communication systems. He has served as Technical Program Committee (TPC) member for multiple conferences and a Reviewer in journals, such as *IEEE COMMUNICATIONS LETTER*, *IEEE TRANSACTIONS ON WIRELESS COMMUNICATIONS*, *Wireless Personal Communications*, *IEEE ACCESS*, *IET Communications*, and *EURASIP Journal on Advances in Signal Processing*. He is an IEEE Communications Society Member and a member of the IEICE Communications Society. He was a co-recipient of the 2019 IEEE LATINCOM Best Paper Award and the 2016 IEEE CONESCAPAN Best Paper Award.



**ISMAEL SOTO** (Senior Member, IEEE) was born in Punta Arenas, Chile. He received the degree in engineering from the University of Santiago of Chile, in 1982, the M.E. degree from University Federico Santa Maria, in 1990, and the Ph.D. degree from the University of Staffordshire, U.K., in 1997. His diverse academic career includes roles in various departments, such as the Department of Computer Science, the Department of Industrial Engineering, and the Department of Electrical

Engineering, University of Santiago of Chile (USACH), Chile. Throughout his career, he has been a Faculty Member with USACH, teaching with the Department of Computer Science, the Department of Industrial Engineering,

and the Department of Electrical Engineering. He is currently an Associate Professor in telecommunications and signal processing with the Department of Electrical Engineering. He has held the position of the National Director and has been an active member of the International Speech Communication Association. His contributions extend to numerous national and international research initiatives, focusing on radio and visible light communication technologies. He is a noted inventor with patents across various countries, and his research interests encompass safety, digital signal processing, visible light communications, and big data analytics. He has played key roles in the professional community, including serving as an International Technical Committee Member for CSNDSP and the Chair of the Organizing Committee for SACVLC. His innovations have earned him an award from the Association of Electrical Engineers (AIE). He has been an Invaluable Reviewer for several prestigious journals, such as *Optimization*, *IET Communications*, and *Optik*, showcasing his extensive expertise and commitment to advancing the field of engineering.



**SANDRA CÉSPEDES** (Senior Member, IEEE) received the B.Eng. degree in telematics engineering and the specialization degree in management of information systems from Universidad Icesi, Colombia, in 2003 and 2007, respectively, and the Ph.D. degree in electrical and computer engineering from the University of Waterloo, Canada, in 2012. She is currently an Assistant Professor with the Department of Computer Science and Software Engineering, Concordia University,

Montreal, Canada. Previously, she was an Associate Professor with the Department of Electrical Engineering, Universidad de Chile, Santiago, Chile, from 2014 to 2021. Since 2020, she has been an Associate Researcher with the Advanced Center of Electrical and Electronic Engineering (AC3E), Valparaíso, Chile. Her research interests include mobile networking and protocol design for the Internet of Things, LEO satellite IoT networks, connected vehicles, and cyberphysical systems. She has served as an Associate Editor for the *IET Communications*, *IEEE INTERNET OF THINGS JOURNAL*, *IEEE Vehicular Technology Magazine*, and *IEEE Internet of Things Magazine*.

...